SCIENCE CHINA Materials ARTICLES

mater.scichina.com link.springer.com Published online 1 April 2024 | https://doi.org/10.1007/s40843-023-2721-5

SPECIAL TOPIC: Biomaterials and Bioinspired Materials

Polysaccharide-based antibacterial nanocomposite hydrogels with Janus structure for treatment of infected extraction socket

Tailong Shi[1†], Yan-Hua Xiong[1†], Weizhuo Song[1], Meizhou Sun[1], Ruonan Wu[1], Yang Li[1], Qiang Sun[2*], Shun Duan[1*] and Fu-Jian Xu[1*]

ABSTRACT **The socket preservation requires special structures for tissue engineering scaffolds. In this study, we developed a kind of Janus nanocomposite hydrogels with antibacterial property, soft tissue barrier function and bone repairing ability using a penetration cross-linking method. The hydrogels were constructed by permeating oxidized sodium alginate solution into a highly viscous nano-hydroxyapatite-contained carboxymethyl chitosan suspension. Through this process, the Janus structure was fabricated. The dense, smooth top-surface showed a significant barrier function against fibroblast cells, while its loose, porous bottom-surface could support bone regeneration with nano hydroxyapatite. And in order to inhibit periodontitis-related bacteria, an antibacterial agent, metronidazole, was combined into the hydrogels. The CAH4M hydrogel showed antibacterial efficiencies of 82% against *S. mutans* and 93% against *P. gingivalis*. The hemolysis ratio was less than 5%, and there was no evident cytotoxicity, demonstrating the good biocompatibility. The *in vivo* anti-infection and bone repairing properties of the hydrogels were verified by a rat model of infected extraction socket. Based on the above results, this study provided a promising strategy to prepare tissue engineering scaffolds that meet clinical requirements for socket preservation and prevention of infection.**

Keywords: polysaccharide, penetration crosslinking, antibacterial, tissue engineering, socket preservation

INTRODUCTION

As a dental treatment, tooth extraction is to remove an irreparably damaged tooth or a tooth that cannot be maintained long-term due to functional or aesthetic reasons. The healing process after tooth extraction involves the formation of blood clots and an epithelial seal over the bone-filled cavities [1–3]. The key process of socket preservation healing is the regeneration of alveolar bone. In the final phase of bone regeneration, remodeling of bone tissue occurs, where immature bone tissue is removed and replaced by mature, organized bone tissue [4,5]. However, after extraction, the width of the alveolar bone typically decreases by 50% within the first year [6–8], and most of the alveolar ridge height is lost within 90 days. The rate of horizontal and vertical bone loss within 6 months after tooth extraction ranges from 29%–63% and 11%–22% [9,10], respectively. Managing the initial alveolar healing after extraction is essential for the healing of the alveolar bone, as it can affect subsequent implantation and restoration treatment.

The management of alveolar healing after tooth extraction has been an important topic in oral surgery research in the past decade, as alveolar bone resorption is a multifactorial biological process that cannot be completely prevented [11]. In response to this situation, treatment is necessary to protect the socket after tooth extraction. And for this purpose, implantation of materials, such as autologous bone grafts, allografts, xenografts, and absorbable or non-absorbable membranes, are used for alveolar bone preservation [12].

Autologous bone grafting is considered the gold standard for implantation [13], but it may cause severe injury at the donor site and is limited by the risk of resorption [14,15]. Allogeneic bone is also limited by source and risk of cross-infection, while xenografts may affect final biological properties due to their different sources and processing methods. Absorbable biofilms have been widely studied due to their advantages, such as a wide source of raw materials, low incidence, and shortened operation time [16] by adding or combining polyphosphate [17], hydroxyapatite [18], metal elements [19], and mRNA [20]. The above-mentioned scaffolds could inhibit bone resorption and promote bone regeneration. However, the low thickness and uniform structure of the membranes could not satisfy the needs of complex extraction socket environments. Based on the above situation, bone powder is filled into the tooth socket before covering the membranes. But it is a complicated process that may increase the risk of periodontitis infection at the root of the alveolar socket, leading to implant failure [21,22], and even inducing infective endocarditis [23,24]. Therefore, it is necessary to develop tissue engineering scaffolds which could provide asymmetric structures of the upper and lower sides. The upper side could prevent invasion of fibroblast, and the lower side could retain the alveolar bone. Compared with commercial resorbable membranes, the filling process might be facile and

[1] State Key Laboratory of Chemical Resource Engineering, Key Lab of Biomedical Materials of Natural Macromolecules (Ministry of Education), Beijing Laboratory of Biomedical Materials, Beijing University of Chemical Technology, Beijing 100029, China
[2] Center of Dental Medicine, China-Japan Friendship Hospital, Beijing 100029, China
[†] These authors contributed equally to this work.
[*] Corresponding authors (emails: superqiangcjf@163.com (Sun Q); duanshun@mail.buct.edu.cn (Duan S); xufj@mail.buct.edu.cn (Xu FJ))

compatible for various shapes of defected areas.

Commonly used tissue engineering scaffold materials are composed of synthetic polymers, including polyurethane [25], polylactic acid [26], poly(caprolactone) [27], poly(amino acid) [28,29], and polyglycolic acid [30]. Compared with synthetic polymers, natural polysaccharides and their derivatives have excellent biocompatibility, biodegradability and hygroscopicity. Furthermore, because of their good film-forming properties, they are used as antibacterial coatings [31,32] and wound dressings [33]. For example, sodium alginate (SA) and chitosan (CS) are representative natural polysaccharides with excellent biocompatibility, plasticity, and cell affinity. However, CS is insoluble in water, which limits its applications. Compared with CS, carboxymethyl CS (CMC) changed the secondary structure of CS due to the introduction of carboxyl groups, which not only destroyed the hydrogen bonds among the molecules of CS, but also increased water solubility by forming carboxylates. Therefore, CMC has high water solubility, good biocompatibility and biosafety properties [34,35]. However, natural polysaccharides often have an unsatisfactory mechanical property to machine due to its complex and irregular structures. They need physical or chemical crosslinking to enhance their properties. After it is modified and cross-linked, its performance has also been further improved [36].

In this work, we constructed hydrogels with a Janus structure through cross-linking of two kinds of natural polymer derivatives, oxidized SA (OSA) and CMC. The polymers were cross-linked through the Schiff base reaction that occurred simultaneously during the interpenetration process between OSA and CMC solutions. In this way, a dense barrier layer could be formed on the upper surface of the hydrogel due to the high crosslink degree, while a loose layer formed on the other side because of the low crosslink degree. And on this basis, combined with the addition of nano-hydroxyapatite (nHA) and antibiotic metronidazole (MTZ), a kind of tissue engineering scaffolds was constructed, which could inhibit the periodontitis-related bacteria and fill the extraction socket to effectively retain the alveolar bone (Scheme 1). The morphology, chemical structures, antibacterial property and biocompatibility were characterized. Furthermore, the *in vivo* anti-infection and bone tissue-repairing performances were evaluated by an animal model of infected extraction socket. The present work provided a new strategy to fabricate Janus-structured hydrogels to barrier against fibroblasts and support osteoblast-related cells simultaneously.

RESULTS AND DISCUSSION

Characterization of Janus nanocomposite hydrogel

The nanocomposite hydrogels were prepared by the crosslinking reaction between the amino groups of CMC and the aldehyde groups of OSA. To determine the aldehyde content of OSA, a hydroxylamine hydrochloride-based titration was performed [37]. The degree of oxidation of OSA was 47.9% (Fig. S1), which was moderate and would not significantly affect the mechanical properties of the hydrogels [38]. Firstly, the CMC-OSA-nHA nanocomposite hydrogels without antibacterial agent were pre-

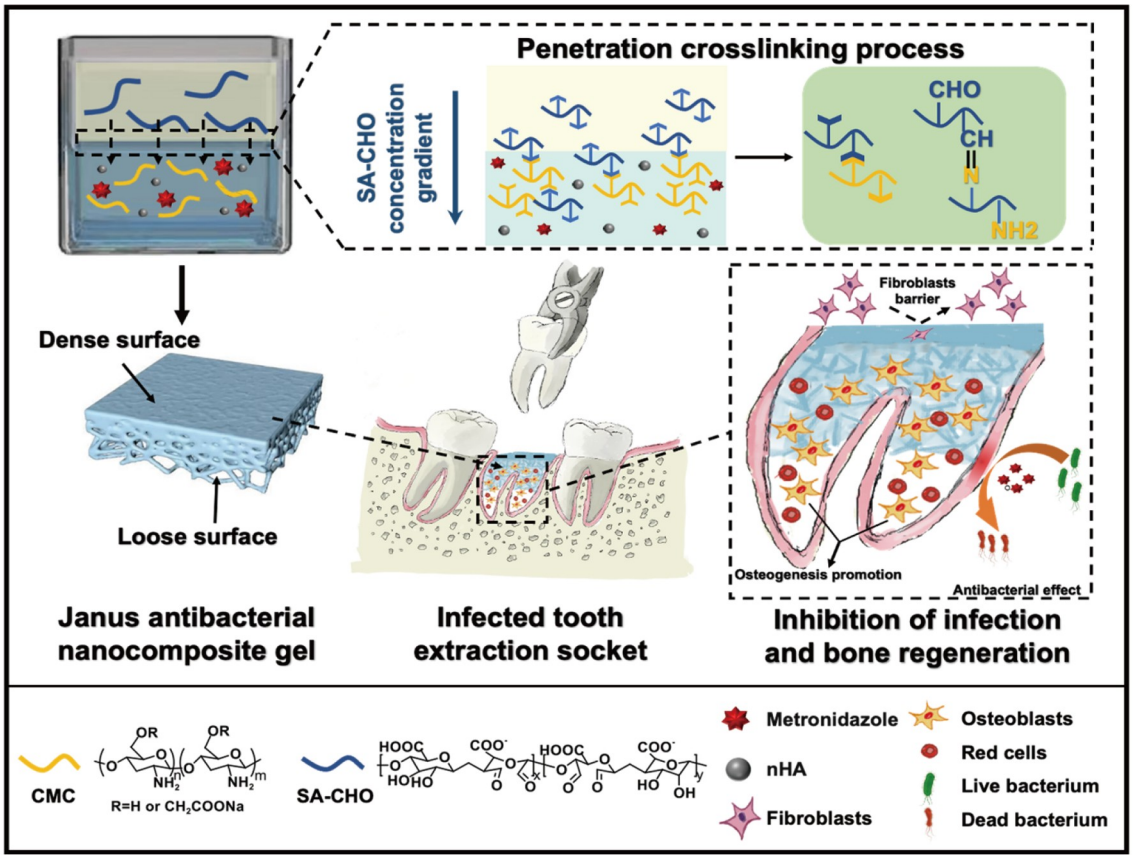

Scheme 1 Preparation of Janus antibacterial nanocomposite hydrogel with antibacterial and tissue repairing properties for the treatment of infected extraction sockets.

pared (denoted as CAH) to study the structure. The morphologies of CAH were observed by scanning electron microscope (SEM, Fig. 1). The upper surface of CAH (Fig. 1a) was dense, which was due to a high crosslinking degree. On the other hand, the lower surface of CAH showed relatively loose, porous structure (Fig. 1b), owing to a lower crosslinking degree. This porous structure is beneficial to regeneration of bone tissue [39]. In addition, the SEM images of cross-section of CAH (Fig. 1c) further demonstrate the Janus structure of CAH.

To characterize the distribution of nHA in the CAH matrix, energy dispersive X-ray spectroscopy (EDS) mappings of phosphorus (P) and carbon (C) were performed (Fig. S2). The results showed that the distribution of the P element (the marker of nHA, yellow signal) was uniform with that of the C element (the marker of polysaccharides, pink signal) from the polysaccharide matrix. From the distribution of the two elements, it was indicated that nHA was uniformly distributed in the matrix, which was due to the hydrophilic property of nHA and its good affinity with the polysaccharide components of CAH. The chemical structures of the hydrogels were also characterized by Fourier transform infrared spectroscopy (FT-IR) (Fig. S3). CMC had a broad peak at 3428 cm^{-1}, which was attributed to the overlapped amino and hydroxyl stretching vibration peaks. The characteristic peaks of CMC at 1598 and 1407 cm^{-1} were owing to the asymmetric stretching vibration of C=O and the bending vibration of N–H and the symmetrical stretching vibration peak of C=O, respectively. The stretching vibration peak of O–H in OSA at 3240 cm^{-1} was significantly wider than that of CMC. Furthermore, the large number of aldehyde groups of OSA could form intermolecular hydrogen bonds with hydroxyl groups, the characteristic peak was broadened. After the formation of the hydrogels, due to the Schiff base reaction between the amino group on CMC and the aldehyde group on OSA, there was a C=N stretching vibration peak at 1640 cm^{-1} in the CAH group. The above-mentioned results demonstrated that CAH hydrogels were crosslinked by CMC and OSA through imine bonds.

For the purpose of eliminate infections by anaerobic bacteria, MTZ solutions with concentrations of 1, 2, and 4 mg mL^{-1} were introduced into the CAH hydrogels, respectively, which were denoted as CAH1M, CAH2M, and CAH4M. Core-level N 1s X-ray photoelectron spectra (XPS) were used to analyze the chemical compositions of the samples. As shown in Fig. S4, the atomic percentages of N element are 9.84% (CAH), 10.31% (CAH1M), 10.44% (CAH2M), and 11.35% (CAH4M) with the increase of MTZ concentrations. This can be attributed to the higher atomic percentage of N element in MTZ compared with CMC. The observed results are consistent with the N element content determined by XPS, and provide evidence for the successful incorporation of MTZ in the gel material. The FT-IR spectra also indicated the MTZ component. In the FT-IR spectra of CAH4M, a characteristic peak at 1520 cm^{-1} was observed, which was attributed to the N–O stretching vibration in $–NO_2$ groups of MTZ.

As the extraction socket is a three-dimensional (3D) defect, the hydrogels used should be capable to fill such defect areas. Therefore, swelling ratios were tested for CAH, CAH1M, CAH2M, and CAH4M, while a commercial guided bone regeneration membrane (GBRM) was taken as a control group. It was observed that all the five samples exhibited saturated water absorption and swelling equilibrium within 20 min (Fig. 2a). Notably, the Janus composite hydrogels (CAH, CAH1M, CAH2M, and CAH4M) exhibited significantly higher swelling ratios than that of GBRM. As shown in Fig. 2b, the Janus composite hydrogels achieved the swelling ratios of approximately 2500% within 24 h, which was about five times higher than that of GBRM. This might be due to their high porosity above 80% (Fig. S5). Such a structure enabled the Janus composite hydrogels to absorb a large amount of water, leading

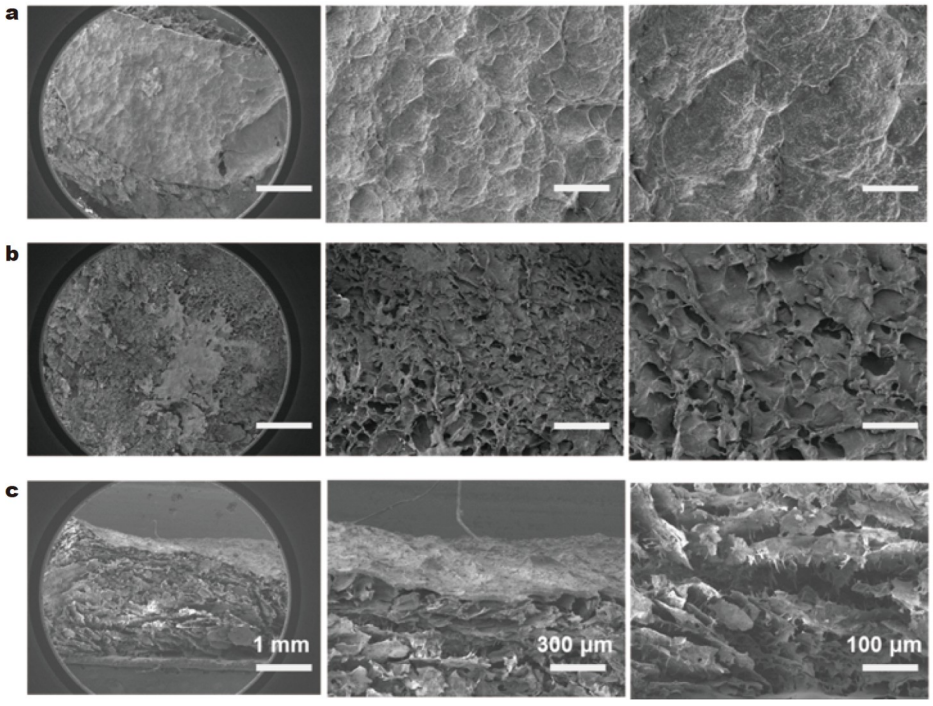

Figure 1 SEM images of CAH. (a) Upper surface; (b) lower surface; (c) cross-section surface.

to volume expansion. The similar porosities of CAH and CAH4M also indicated that the crosslinking degrees of the two kinds of hydrogels were not significantly different. The high swelling ratio of the Janus composite hydrogels might absorb blood effectively, promote local coagulation, and expand the volume to fill the cavity of the extraction socket. In addition, the rheological analysis demonstrated the modulus of CAH and CAH4M was about 3 kPa (Fig. S6).

In order to be effective for bone repair, the hydrogels should have suitable degradation profiles that are able to degrade gradually to provide spaces for newly formed bone tissue [40]. Therefore, the degradation behaviors of Janus composite hydrogels were investigated. The degradation rates of Janus hydrogels with four different contents of MTZ were similar (Fig. 3a), with a significant declined masses within 7 d and a gradually flat tendencies in the later period. However, the degradation rate of GBRM was slower than that of the Janus composite hydrogel within 4 d, but became faster in the later period. This phenomenon might be due to the loose structure of the Janus composite hydrogel with a low crosslinking degree. The upper part of the Janus composite hydrogel had high crosslinking degree and dense structure, resulting in a slow degradation rate in the later stage. On the other hand, the double-layer collagen bioabsorbable membrane, GBRM, was lack of cross-linking structure. The structure of GBMR became looser with degradation time, resulting in an accelerated degradation rate [41]. After 28 d of degradation, the Janus composite hydrogels retained nearly 60% of their mass, while the GBRM only had about 20% of it (Fig. 3b), which showed that the chemical stability of the Janus composite hydrogels was higher than that of GBRM. Bone regeneration is a long-term process which needs a slow degradation profile to match the timing of alveolar bone healing in the socket. Moreover, the morphology of the CAH4M and GBRM samples was observed during the degradation test. At 1 d, the surface morphology of CAH4M and GBRM both showed a dense state. With the prolongation of degradation time, the surface of CAH4M was still dense, while GBRM had obvious cracks at 14 and 28 d (Fig. S7). This result proved the stability of the dense structure of the upper layer of CAH4M, which could provide a barrier against soft tissues and a space for bone regeneration. On the contrary, epithelial and fibroblast cells might migrate across GBRM through the cracks and occupy the extract socket. These results indicated that CAH Janus composite hydrogels are more stable than GBRM for socket preservation.

In vitro antibacterial properties and biocompatibility

The oral cavity connects the external environment with continual exposure of various types of bacteria. After tooth extract operation, bacterial invasion might induce severe infections [42]. *S. mutans* and *P. gingivalis* are common pathogens that induce oral infections [43,44]. Therefore, materials for socket preservation should possess potent bactericidal abilities, especially against anaerobic bacteria. For this purpose, a kind of antibiotics against anaerobic bacteria, MTZ, was introduced into CAH Janus hydrogels. Due to the rapid release profile of MTZ from

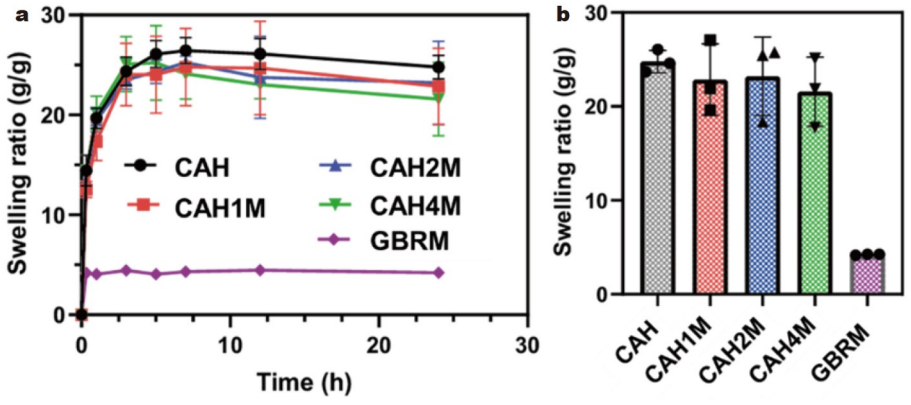

Figure 2 (a) Swelling ratio curves within 1 d and (b) the equilibrium swelling ratios of CAH, CAH1M, CAH2M, CAH4M, and GBRM at 1 d.

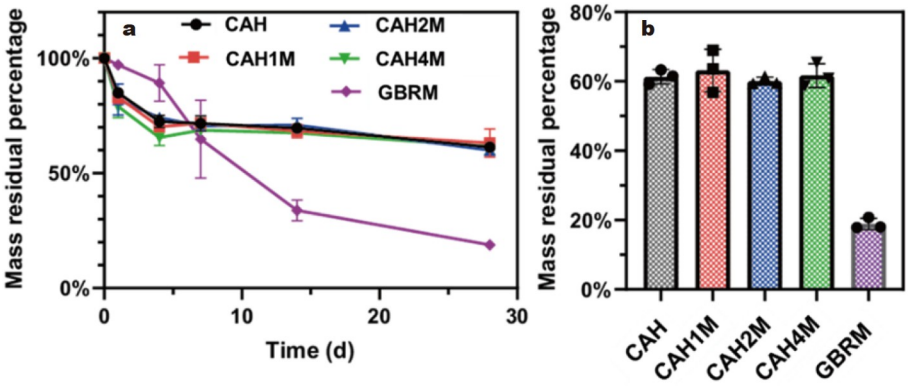

Figure 3 (a) Degradation profiles and (b) the final residual mass ratios at 28 d.

CAH4M (Fig. S8), it showed a significant antibacterial effect against both *S. mutans* and *P. gingivalis* (Fig. 4a, b). The bactericidal efficiencies against *S. mutans* and *P. gingivalis* of CAH4M were 82% and 93%, respectively. These bactericidal efficiencies could guarantee the high anti-infection performances of CAH4M.

Since tooth extraction often causes bleeding, the hemocompatibility is crucial. To assess the hemolysis ratio, erythrocyte suspensions were co-cultured with the samples for 3 h. The results showed that the hemolysis ratios of CAH, CAH1M, CAH2M, and CAH4M were all lower than 5%, which demonstrated that Janus composite hydrogels had high hemocompatibility (Fig. 4c). In addition, the cytotoxicity was also evaluated with mouse fibroblast (L929) cells and rat bone marrow mesenchymal stem cells (BMSC). As shown in Fig. 4d, e, CAH Janus composite hydrogels containing different amounts of MTZ did not exhibit significant cytotoxicity. The primary reason for the good *in vitro* biocompatibility is due to the main component. The Janus composite hydrogels were composed of natural polysaccharide derivatives.

Fibroblast barrier properties

There is a growth competition between soft tissue and bone tissue in the extraction socket. Unfortunately, the growth rate of bone tissue is much slower than that of soft tissue [16]. Therefore, materials for socket preservation should block the growth of soft tissue into the socket to allow bone tissue regeneration. In this study, L929 cells were used to assess the barrier properties of the Janus composite hydrogel. The cells were seeded on the dense surface of CAH4M and cultured for 4 d. Cell distribution was observed by fluorescent staining to evaluate if the cells could migrate across the dense surface of the Janus composite hydrogel. 3D images through the *z*-axis scanning show that the cells were still distributed on the dense surface after 4 d (Fig. 5). These results demonstrated the unique structure of Janus composite hydrogel had the function as a cell barrier, which was

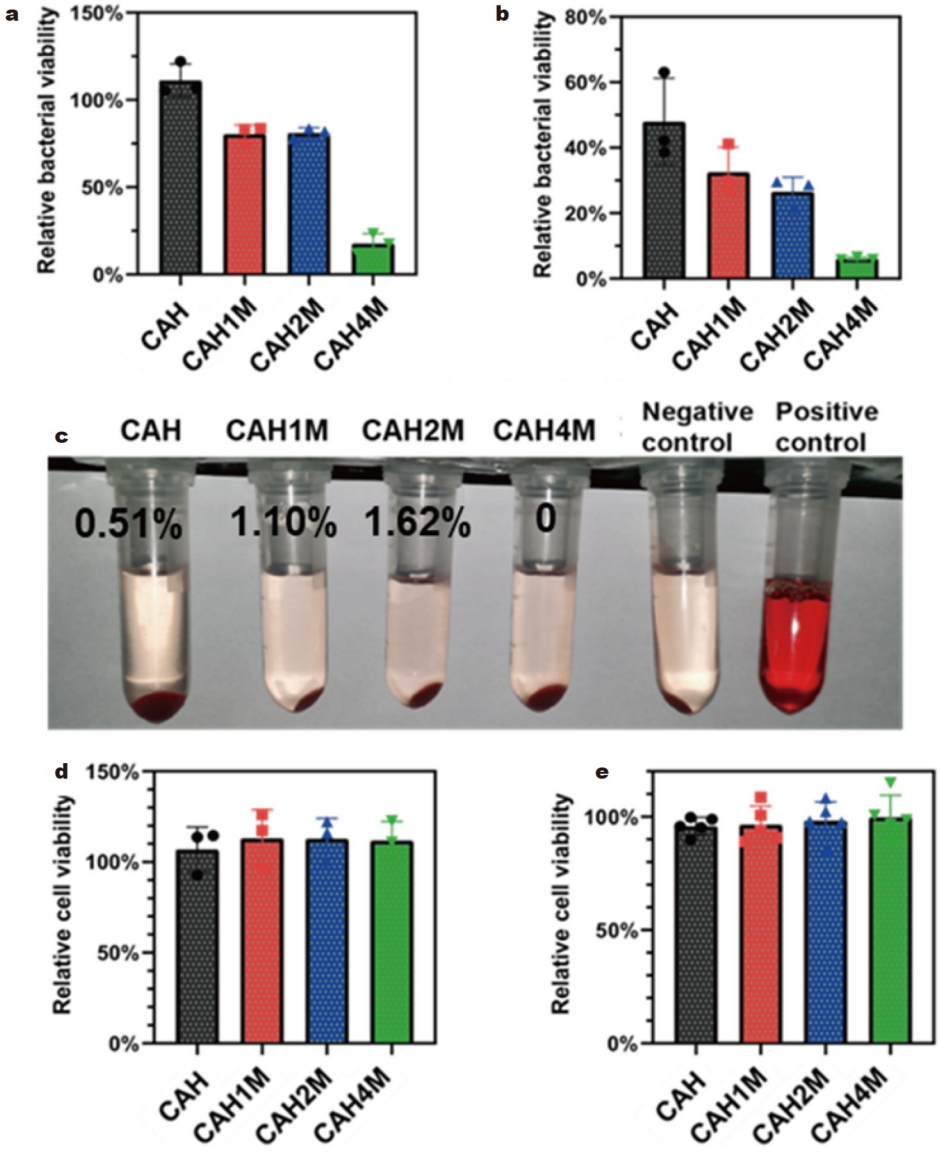

Figure 4 Antibacterial efficiencies against *S. mutans* (a) and *P. gingivalis* (b); (c) hemolysis ratios; cytotoxicity against L929 cells (d) and BMSC (e).

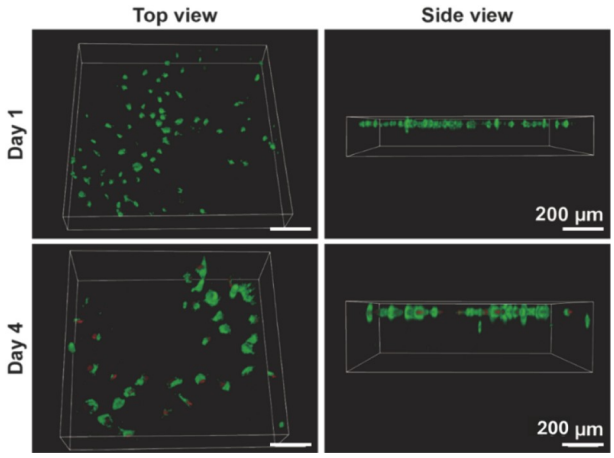

Figure 5 3D images of L929 cells on the dense side of CAH4M at 1 and 4 d.

beneficial for reserving the space for bone tissue growth. Owing to its excellent biocompatibility, the ability to eliminate anaerobic bacteria and barrier property against fibroblasts, CAH4M was selected for *in vivo* study.

In vivo performance of CAH4M for the treatment of tooth extraction socket infection in rats

First, a rat model of tooth extraction socket infection was surgically constructed. After anesthetization, the area around its upper right incisor was exposed, and the tooth was completely extracted without affecting the left upper incisor (Fig. S9). The success of the extraction was determined by the shape and length of the extracted tooth (Table S1). Then, 10 μL of *P. gingivalis* suspensions with the density of 10^8 CFU mL^{-1} were added into the sockets, followed by filling samples of CAH, CAH4M, and GBRM, respectively. The group that was inoculated by bacteria without any materials (W/O group) and the group that received neither bacteria nor materials (Control group) were taken as controls. Finally, the cavities were closed and sutured to complete the establishment of the animal model.

At 4 week, the CAH4M group showed the best recovery of soft tissues at the operation sites, which is similar to the Control group (Fig. 6a), preliminary proving the *in vivo* anti-infection property of CAH4M. Subsequently, infection and bone regeneration at the extraction socket were further assessed by hematoxylin and eosin (H&E) staining. As shown in Fig. 6b, there was a noticeable inflammatory response in the socket at 1 week of the W/O group, CAH group, and GBRM group, which was characterized by a large number of inflammatory cells. In contrast, in the CAH4M group, the inflammatory response was inhibited significantly. At 4 week, a large number of osteoblasts were observed in the CAH4M group, indicating regeneration process of alveolar bone at the extraction socket. The results of H&E staining revealed that CAH4M could suppress the local inflammatory response caused by bacteria effectively in the early stage, and promote bone formation in the later stage, which was more effective than GBRM. On the other hand, the Janus-structured hydrogels comprised of derivatives of natural polysaccharides, which possessed high compatibility. Thus, soft tissues could proliferate on the surface of the dense surface. These results demonstrated CAH4M had good *in vivo* performances of anti-infection and socket preservation.

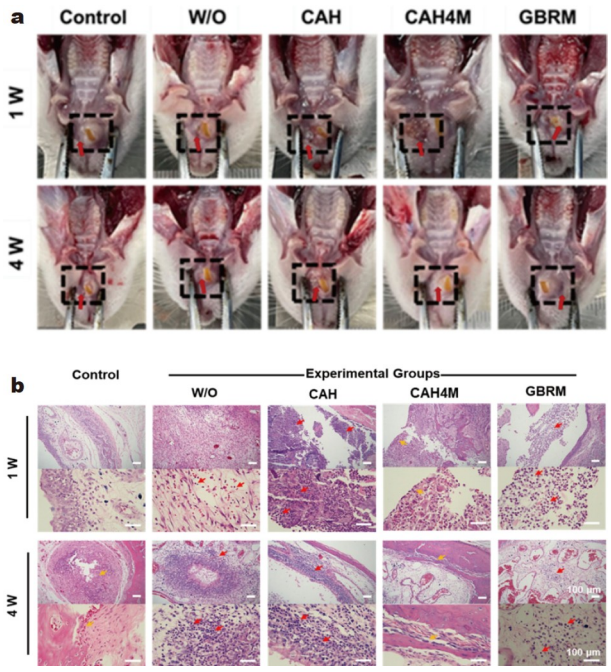

Figure 6 (a) General views of the soft tissues above extraction sockets at 1 and 4 week after surgery; (b) H&E staining images of the tissues around socket preservation (red arrows: inflammatory cells; yellow arrows: osteoblasts).

CONCLUSIONS

In this study, a Janus composite hydrogel was developed. The unique asymmetric structure had a dense surface that served as a barrier to fibroblasts and a porous part that supported bone growth. This structure as well as the high swelling ratio made it an ideal material for socket preservation. The degradation rate of such hydrogels fits the growth of bone tissue. Additionally, the combination with MTZ endowed the hydrogels with effective antibacterial properties, against anaerobic bacteria. The good hemocompatibility and cytocompatibility made CAH4M promising for *in vivo* application. In the animal experiment, CAH4M showed outstanding anti-infection property, and could induce bone regeneration at the socket site. This study provided a kind of potential materials for prevent and treatment of infected socket preservation.

Received 19 September 2023; accepted 8 December 2023; published online 1 April 2024

1 Buser D, Chappuis V, Belser UC, *et al.* Implant placement post extraction in esthetic single tooth sites: When immediate, when early, when late? Periodontol 2000, 2000, 73: 84–102
2 Moran IJ, Richardson L, Heliotis M, *et al.* A bleeding socket after tooth extraction. BMJ, 2017, 357: j1217
3 Pihlstrom BL, Michalowicz BS, Johnson NW. Periodontal diseases. Lancet, 2005, 366: 1809–1820
4 Araújo MG, Silva CO, Souza AB, *et al.* Socket healing with and without immediate implant placement. Periodontol 2000, 2019, 79: 168–177
5 Araújo MG, Dias DR, Matarazzo F. Anatomical characteristics of the alveolar process and basal bone that have an effect on socket healing. Periodontol 2000, 2023, 93: 277–288
6 Johnson K. A study of the dimensional changes occurring in the maxilla following tooth extraction. Aust Dent J, 1969, 14: 241–244
7 Araújo MG, Lindhe J. Ridge alterations following tooth extraction with

and without flap elevation: An experimental study in the dog. Clin Oral ImPlants Res, 2009, 20: 545–549
8 Cardaropoli G, Araújo M, Hayacibara R, *et al.* Healing of extraction sockets and surgically produced—augmented and non-augmented—defects in the alveolar ridge. An experimental study in the dog. J Clinic Periodontol, 2005, 32: 435–440
9 Fickl S, Zuhr O, Wachtel H, *et al.* Tissue alterations after tooth extraction with and without surgical trauma: A volumetric study in the beagle dog. J Clinic Periodontol, 2008, 35: 356–363
10 Schropp L, Wenzel A, Kostopoulos L, *et al.* Bone healing and soft tissue contour changes following single-tooth extraction: A clinical and radiographic 12-month prospective study. Int J Periodon Rest Dent, 2003, 23: 313–323
11 Avila-Ortiz G, Chambrone L, Vignoletti F. Effect of alveolar ridge preservation interventions following tooth extraction: A systematic review and meta-analysis. J Clinic Periodontol, 2019, 46: 195–223
12 Alfonsi F, Borgia V, Iezzi G, *et al.* Molecular, cellular and pharmaceutical aspects of filling biomaterials during the management of extraction sockets. Curr Pharm Biotechnol, 2017, 18: 64–75
13 Yamamichi N, Itose T, Neiva R, *et al.* Long-term evaluation of implant survival in augmented sinuses: A case series. Int J Periodon Rest Dent, 2008, 28: 163–169
14 Pikdöken L, Gürbüzer Bı, Küçükodacı Z, *et al.* Scintigraphic, histologic, and histomorphometric analyses of bovine bone mineral and autogenous bone mixture in sinus floor augmentation: A randomized controlled trial—Results after 4 months of healing. J Oral Maxillofac Surg, 2011, 69: 160–169
15 Maria Soardi C, Spinato S, Zaffe D, *et al.* Atrophic maxillary floor augmentation by mineralized human bone allograft in sinuses of different size: An histologic and histomorphometric analysis. Clin Oral ImPlants Res, 2011, 22: 560–566
16 Kühl S, Götz H, Hansen T, *et al.* Three-dimensional analysis of bone formation after maxillary sinus augmentation by means of micro-computed tomography: A pilot study. Int J Oral Maxill Implan, 2010, 25: 930–938
17 Gu J, Jiao K, Li J, *et al.* Polyphosphate-crosslinked collagen scaffolds for hemostasis and alveolar bone regeneration after tooth extraction. Bioactive Mater, 2022, 15: 68–81
18 Ou M, Huang X. Influence of bone formation by composite scaffolds with different proportions of hydroxyapatite and collagen. Dent Mater, 2021, 37: e231–e244
19 Tian B, Li X, Zhang J, *et al.* A 3D-printed molybdenum-containing scaffold exerts dual pro-osteogenic and anti-osteoclastogenic effects to facilitate alveolar bone repair. Int J Oral Sci, 2022, 14: 1–8
20 Li X, Li S, Qi H, *et al.* Early healing of alveolar bone promoted by microRNA-21-loaded nanoparticles combined with Bio-Oss particles. Chem Eng J, 2020, 401: 126026
21 Rosenquist B, Grenthe B. Immediate placement of implants into extraction sockets: Implant survival. ImPlant Dent, 1996, 5: 297
22 Quirynen M, Gijbels F, Jacobs R. An infected jawbone site compromising successful osseointegration. Periodontol 2000, 2003, 33: 129–144
23 Kinane DF, Stathopoulou PG, Papapanou PN. Periodontal diseases. Nat Rev Dis Primers, 2017, 3: 17038
24 Wu Y, Lin Y, Cong Z, *et al.* Peptide polymer-doped cement acting as an effective treatment of MRSA-infected chronic osteomyelitis. Adv Funct Mater, 2022, 32: 2107942
25 Vellayappan MV, Duarte F, Sollogoub C, *et al.* Fabrication of architectured biomaterials by multilayer co-extrusion and additive manufacturing. Adv Funct Mater, 2023, 33: 2301547
26 Ko KW, Park SY, Lee EH, *et al.* Integrated bioactive scaffold with polydeoxyribonucleotide and stem-cell-derived extracellular vesicles for kidney regeneration. ACS Nano, 2021, 15: 7575–7585
27 Ovsianikov A, Khademhosseini A, Mironov V. The synergy of scaffold-based and scaffold-free tissue engineering strategies. Trends Biotechnol, 2018, 36: 348–357
28 Wu Y, Chen K, Wang J, *et al.* Host defense peptide mimicking antimicrobial amino acid polymers and beyond: Design, synthesis and biomedical applications. Prog Polym Sci, 2023, 141: 101679
29 Zhong C, Wu Y, Lin H, *et al.* Advances in the antimicrobial treatment of osteomyelitis. Compos Part B-Eng, 2023, 249: 110428
30 Lee SS, Du X, Kim I, *et al.* Scaffolds for bone-tissue engineering. Matter, 2022, 5: 2722–2759
31 Zhang L, Hu C, Sun M, *et al.* Bodipy-functionalized natural polymer coatings for multimodal therapy of drug-resistant bacterial infection. Adv Sci, 2023, 10: 2300328
32 Zhang L, Yang Y, Xiong YH, *et al.* Infection-responsive long-term antibacterial bone plates for open fracture therapy. Bioactive Mater, 2023, 25: 1–12
33 Wu J, Pan Z, Zhao ZY, *et al.* Anti-swelling, robust, and adhesive extracellular matrix-mimicking hydrogel used as intraoral dressing. Adv Mater, 2022, 34: 2200115
34 Liu F, Liu X, Chen F, *et al.* Mussel-inspired chemistry: A promising strategy for natural polysaccharides in biomedical applications. Prog Polym Sci, 2021, 123: 101472
35 Upadhyaya L, Singh J, Agarwal V, *et al.* Biomedical applications of carboxymethyl chitosans. Carbohydrate Polyms, 2013, 91: 452–466
36 Chen L, Peng M, Zhou J, *et al.* Supramolecular photothermal cascade nano-reactor enables photothermal effect, cascade reaction, and *in situ* hydrogelation for biofilm-associated tooth-extraction wound healing. Adv Mater, 2023, 35: 2301664
37 Emami Z, Ehsani M, Zandi M, *et al.* Controlling alginate oxidation conditions for making alginate-gelatin hydrogels. Carbohydrate Polyms, 2018, 198: 509–517
38 Xiong YH, Zhang L, Xiu Z, *et al.* Derma-like antibacterial polysaccharide gel dressings for wound care. Acta Biomater, 2022, 148: 119–132
39 Jiang SJ, Wang MH, Wang ZY, *et al.* Radially porous nanocomposite scaffolds with enhanced capability for guiding bone regeneration *in vivo*. Adv Funct Mater, 2022, 32: 2110931
40 Wei S, Ma JX, Xu L, *et al.* Biodegradable materials for bone defect repair. Military Med Res, 2020, 7: 54
41 Kong HJ, Alsberg E, Kaigler D, *et al.* Controlling degradation of hydrogels *via* the size of crosslinked junctions. Adv Mater, 2004, 16: 1917–1921
42 Lockhart PB, Brennan MT, Sasser HC, *et al.* Bacteremia associated with toothbrushing and dental extraction. Circulation, 2008, 117: 3118–3125
43 Sun Z, Ma L, Sun X, *et al.* The overview of antimicrobial peptide-coated implants against oral bacterial infections. Aggregate, 2023, 4: e309
44 Kuboniwa M, Houser JR, Hendrickson EL, *et al.* Metabolic crosstalk regulates Porphyromonas gingivalis colonization and virulence during oral polymicrobial infection. Nat Microbiol, 2017, 2: 1493–1499

Acknowledgements This work was supported by the National Key Research and Development Program of China (2022YFC2403200), the National Natural Science Foundation of China (52221006, 52293382, 52122304, and 52073024), the National High Level Hospital Clinical Research Funding (2023-NHLHCRF-YGJH-ZR-02), and Beijing Outstanding Young Scientist Program (BJJWZYJH01201910010024).

Author contributions Xu FJ, Duan S, and Sun Q proposed the idea of this work. Shi T wrote the manuscript with support from Song W, Sun M, and Wu R. Xiong YH and Song W performed the experiments and organized the figures. The manuscript was discussed and revised by all authors.

Conflict of interest The authors declare that they have no conflict of interest.

Supplementary information Experimental details and supporting data are available in the online version of the paper.

Tailong Shi received his BS degree in functional materials from Beijing University of Chemical Technology (2022). He is currently a master candidate at Beijing Laboratory of Biomedical Materials, Beijing University of Chemical Technology under the supervision of Prof. Fu-Jian Xu. His research activities focus on antibacterial dressings.

Yan-Hua Xiong received his PhD degree in materials science and engineering from Beijing University of Chemical Technology (2022). He is currently a technical manager at IMEIK Technology Development Co., Ltd. His research activities focus on the construction of tissue scaffolds and the regeneration of soft tissues.

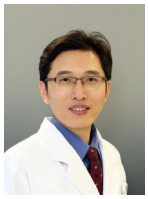

Qiang Sun graduated from the Dental School of China Medical University and is an associate professor of Peking University. He attended the international postdoc scholarship at the University of Pennsylvania Program. His research interests include but not limited to bone osteogenesis with innovative methods and antibiotic therapy with medical dressings loaded by medicine.

Shun Duan graduated from Qingdao University of Science and Technology, majoring in pharmaceutical engineering/English, with a bachelor's degree of engineering and a bachelor's degree of arts. In 2014, he graduated from Beijing University of Chemical Technology with a PhD degree majoring in materials science and engineering. His main research interest is antibacterial materials, which combines active polymerization with natural polymers. He performs a series of researches in novel antimicrobial materials, controllable surface functionalization of medical materials and industrialization of antimicrobial materials.

Fu-Jian Xu obtained PhD degree in biomolecular engineering in 2006 from the National University of Singapore (NUS). After two-years of post-doctoral work as a Lee Kuan Yew Postdoctoral Fellow in NUS, he joined Beijing University of Chemical Technology in 2009. His research interests focus on functional biomacromolecules.

具有Janus结构的多糖基抗菌纳米复合水凝胶用于治疗拔牙窝感染

史泰龙[1†], 熊彦华[1†], 宋炜卓[1], 孙美州[1], 吴若楠[1], 李杨[1], 孙强[2*], 段顺[1*], 徐福建[1*]

摘要 拔牙窝位点保存需要特殊的组织工程支架. 在本研究中, 我们采用渗透交联的方法开发了一种具有抵抗成纤维细胞入侵、牙槽骨保存和抗菌的多功能Janus结构复合水凝胶. 通过将氧化的海藻酸钠溶液渗透到含有羧甲基壳聚糖的高黏性纳米羟基磷灰石悬浮液中来构建水凝胶. 通过这个过程制备出的Janus结构水凝胶, 其致密、光滑的上表面对成纤维细胞显示出显著的屏障功能, 而其疏松、多孔的下表面可以在纳米羟基磷灰石的作用下进行有效的牙槽骨保存, 并且在水凝胶中加入了一种抗菌剂甲硝唑, 有效抑制了牙周炎相关细菌. 其中最优组CAH4M水凝胶对变形链球菌和牙龈卟啉单胞菌的抗菌效率分别为82%和93%, 溶血率小于5%, 没有明显的细胞毒性.